Development and application of a porous cage carrier method for detecting trace elements in soils by direct current glow discharge mass spectrometry

Article (Accepted Version)

ARTICLE

Development and application of a porous cage carrier method for detecting trace elements in soils by direct current glow discharge mass spectrometry

Received 00th January 20xx,
Accepted 00th January 20xx

DOI: 10.1039/x0xx00000x

Jiangli Dong,[a,d] Rong Qian,*[a] Shangjun Zhuo,[a] Pengfei Yu,[c] Qiao Chen,[b] and Zhongquan Li,[a]

The accurate and reliable determination of trace elements in soil still remains a big challenge for glow discharge mass spectrometry due to the poor conductive nature of soils. In the present work, a porous cage carrier was developed and applied into the analysis of soils. The investigation results suggested that the carrier with circular cross-section area in the range from 20 to 38 mm^2, length from 15 to 17 mm and diameter of hole size from 1.5 mm to 2.0 mm could obtain good signals. Then the porous cage carrier method was systematically evaluated with analysing three types of soil reference materials. The discharge process was maintained stable more than 100 minutes, which was much longer than boric acid method and indium sheet method. The investigations suggested that the internal precision was obtained within 16%, the external precision was better than 20% and the relative error was in the range from 0.7% to 17%. The detection limit of Tb could reach 0.014 μg g^{-1}, which made the new method qualified for the analysis of trace elements in soils. Compared to the traditional tablet-pressed methods, the porous cage carrier method was investigated not only convenient for sample preparation, but also indicated good stability, reproducibility and better detection limit for trace elements. Furthermore, this method was proved to have potential application of GD-MS in the environmental area.

1. Introduction

The public concern regarding environmental pollution has been increasing rapidly over recent decades. It is well-known that trace elements are one of the main sources of pollution in the environment, because of their significant effect on its ecological quality.[1-3] Trace elements resulted from atmospheric and industrial pollution accumulate in the soil, and influence the ecosystem nearby. For example, trace elements, such as rare earth elements (REEs) have a positive effect on photosynthesis and water use efficiency by plants,[4,5] but excessive concentrations of REEs would cause bioaccumulation in biota, and chronic toxicity.[6,7] Hence, the accurate and reliable determination of trace elements in soil is vital of importance in the point of environmental pollution.

Atomic spectrometry (AES/AAS),[8] inductively coupled plasma mass spectrometry (ICP-MS),[9-11] instrumental neutron activation analysis (INNA),[12,13] X-Ray fluorescence spectrometry (XRF),[14] laser ablation inductively coupled plasma mass spectrometry (LA-ICP-MS)[15] and glow discharge mass spectrometry (GD-MS)[16-22] has been used in geology and geochemistry surveys. However, due to the refractory nature of the soil samples, the sample preparation is time-consuming with the risk of sample contamination from chemical reagents in dissolve process when utilizing the conventional solution-based approaches, such as ICP. In addition, for determination of some trace elements by INNA, a long irradiation time is required. Therefore, direct analytical methods, such as XRF, GD-MS and LA-ICP-MS and so on, are inclined to be chose for replacement. Unfortunately, XRF and LA-ICP-MS does not have sensitive detection limits of most trace elements. Comparatively, GD-MS has its merits including low detection limits, high sensitivity, high mass resolution and the capability to analyze elements across the periodic table from major compositions to trace compositions, over a wide dynamic range (ng g^{-1} to 100%).[23-27]

Early experiment studies on soils by GD-MS were mainly attempted in Oak ridge national lab. The potential feasibility of analyzing soils by GD-MS was firstly verified through the direct measurement of the uranium isotopic abundances in soils with fair accuracy.[16] After then, its analytical capabilities of identification and quantification for multi-elements in soils were evaluated by using reference samples.[17] Furthermore, a single set of relative sensitivity factors (RSF) values for quantitative analysis of soils were developed and the influence of oxygen content, conducting host matrix, and soil

[a] National Center for Inorganic Mass Spectrometry in Shanghai, Shanghai Institute of Ceramics, Chinese Academy of Sciences, 1295 Ding Xi Road, Shanghai 200050, People's Republic of China.
[b] Department of Chemistry, School of Life Sciences, University of Sussex, Brighton BN1 9QJ, United Kingdom.
[c] Shanghai Institute of Microsystem and Information Technology, Chinese Academy of Sciences, 865 Changning Road, Shanghai 200050, People's Republic of China.
[d] Center of Materials Science and Optoelectronics Engineering, University of Chinese Academy of Sciences, Beijing, China.

composition on RSF values was examined.[18] Based on the previous studies, the effect of interferences from the blending materials, the secondary cathode, the discharge gas and the matrix on the sensitivity of the GD-MS were investigated by Maria Betti etc. from Germany, where detection limits combined with mass resolution were taken into account for further application in soils analysis.[19] However, much more investigations still need to be performed to improve the detection limits for the wider number of isotopes with more acceptable resolution and shorter integrated time for widespread application. The major obstacle to application results from the poor conductive nature of soils. The most widely adopted method in previous studies is to compact the soil with high purity metal (such as aluminium, silver, copper and tantalum and so on) as a conductive binder to form a pin or plate-shaped cathode.[16-18, 21] However, the soils are hard to be mixed with conductive binder uniformly to form pin or plate-shaped cathodes with a certain mechanical strength, the process of which is often time-consuming and easy to bring in secondary contamination. The second approach is to cover a metallic secondary cathode diaphragm at the surface of the soil plate, allowing the surface covered by a thin metallic layer during sputtering.[19] However, soil sample still has difficulty in molding due to its incompact nature. Apart from the two, radiofrequency (rf) powered GD might hold promise of direct soil analysis.[20] Unfortunately, rf-GD-MS instrument is still an unusual method and only a few are commercially available. Different conventional sample preparation methods have been tried to analyze soils in our lab. The unacceptable signal intensity related to the lower detection limit as well as poor stability were found to be another two obstructions even if the issue on sample preparation were solved. Therefore, an easier established method for soil analysis by GD-MS with more convenient sample preparation, better detection limits and good stability is eager to be developed.

In this study, a porous cage carrier method was developed based on our previous work[28,29] to meet all the above demands. In this method, porous cage carrier was fabricated with high purity tantalum plate drilled by laser. The influence of geometric and dimensional factors including cross-section shape, length and width as well as hole size involved porosity of the cage on the signal intensity was studied, where the binary oxide SiO_2 and Al_2O_3 were used as references. Then the cage carrier with optimized parameters was used to analyze soils. Three kinds of soil reference materials were used to validate the stability, reproducibility, accuracy and detection limits of this method. With such configuration, this porous cage carrier method was not restricted by the geometric shape of the sample. The introduced sample needed only a small amount of soils matching the carrier size, which could be apparently implementable by rough mechanical press. Furthermore, this porous cage carrier method could also improve the stability and detection limits. The method will promote the further application of GD-MS in the environmental area.

2. Experimental

2.1 dc-GD-MS experiments

All the experiments were performed with an AutoConcept GD90 glow discharge mass spectrometer (Mass Spectrometry Instruments Ltd., U.K.), which was a double-focusing magnetic sector instrument with reverse Nier-Johnson configuration. The discharge cell used was designed to accept pin-shaped samples, and the cell was pre-cooled by liquid nitrogen to reduce the background noise due to residual gases. The glow discharge was supported with high purity (>99.9999%) argon. The signal of the ion beams was detected by a Daly detector with the current in the range from 10^{-19} to 10^{-13} A, while a Faraday cup with the current in the range from 10^{-13} to 10^{-9} A. A resolution of about 3000 (m/△m) was utilized, which was adequate to resolve interferences from most isotopes.

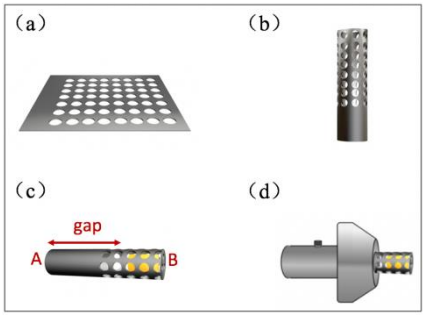

Fig. 1 The schematic diagram for the fabrication of porous cage carrier (a) the porous tantalum sheets, (b) the fabricated porous cage carrier, (c) the porous cage carrier filled with soil sample and (d) the prepared sample to be analyzed by dc-GD-MS analysis.

2.2 Fabrication of porous cage carrier

The porous cage carriers used in this study were all made of ultrahigh pure tantalum sheets (99.999%, Goodfellow Cambridge Limited). Tantalum would be used in priority in this study because of its lower sputter rate, the limited interference with rare earth elements and matrix Si in soils (see also the detailed discussion in section 3.4.1). The tantalum sheets in thickness of 0.25 mm were firstly perforated by laser into porous patterns with different circular hole sizes (Fig. 1(a)). Then the porous tantalum sheets were made into cage carriers with different length and cross-section in different geometric shape and different area (Fig. 1(b)). As shown in Fig.1(c), about one third part of tantalum carrier started from the end A of the porous cage carrier was not drilled by laser, making it easily to be fixed on the sample holder by screw. The head at the other end B of the cage could be opened to load the samples. Since the stability of the fit might be a key factor in the plasma operation stability, the soil samples were previously manufactured into the proper size to fit cage to keep the enough contacting with the inner surface of the cage. Sometimes, if the sample was small, we put some tantalum strips between the gap of the sample and end A to ensure the sample held in the cage steady.

2.3 Sample preparation and measurement conditions

SiO_2 and Al_2O_3 ceramics, which were provided by Shanghai Institute of Ceramics, Chinese Academy of Sciences, were used to assess the influence of the geometric parameters of the carrier on the signal intensity. SiO_2 and Al_2O_3 were chosen as reference samples because they are binary oxides and have limited matrix composition. All the samples and porous cage carriers were cleaned with dilute nitric acid solution, followed by washing in anhydrous ethanol with an ultrasonic cleaner and drying with a hot-air blower, and finally plasma etched for 15 mins in the GD source prior to mass spectrometric analysis. The pre-etching was carried out using a discharge voltage of 2.0 kV and a discharge current of 1.8 mA. The data presented in this study were average values of five determinations in half an hour.

Three geological reference materials GBW07401, GBW07430 and GBW07390, which were certified by National Research Center for Certified Reference Materials in China, were used to evaluate the stability, accuracy and detection limits of the porous cage carrier method. The certified values of trace elements in GBW07401, GBW07430 and GBW07390 are listed in Table 1 and Table 2. Before analysis, all the soil samples were dried at 105 ℃ for 2 h. This temperature was chosen to drive off water without the excessive loss of volatile elements. The soil powder was then pressed at 2×10^6 Pa. It should be emphasized here that the perfect forming is not overcritized, as the fragments can also meet the testing condition benefited from the carrier design as shown in Fig. 1(c). The easy-handled procedure without further sample preparation is time-saving. Signal of the soils was collected after pre-sputtering at 2.0 kV and 1.8 mA for 20 mins.

In order to investigate the advantages of the porous cage carrier method, two conventional methods by using Boric acid (Sinopharm Chemical Reagent Co., Ltd, China) and ultrapure indium (99.9999%, Emei Semiconductor Material Factory & Institute, Sichuan, China) to form the sample tablets, respectively, were introduced to analyze the soils for comparison.

3. Results and discussion

3.1 Analysis of impurities of porous cage carrier

At the beginning of our experiment, a cylindrical cage carrier with Φ2.0 mm holes in the dimension of Φ5 mm × 15 mm was selected to analyze its impurities. The porous cage carrier was pre-sputtered for 15 mins before collecting signal. From the panoramic analysis, only the concentration of niobium (Nb) was about 3.2 μg g^{-1} (relative to Ta), while other elements were below the level of 0.3 μg g^{-1} (relative to Ta). Especially for rare earth elements, the concentrations were below the level of 2ng g^{-1} (relative to Ta). These results indicated that the purity of the Ta carrier was good enough for our experiments.

3.2 Influence of the geometric parameters of the carrier on the signal intensity

At the beginning of this study, the influence of the shape and area of the cross-section on the signal intensity were investigated by using SiO_2 and Al_2O_3. The carriers with the circular and square cross-section in the area of 7.01, 19.63, 38.47 and 63.59 mm^2 were fabricated respectively. As shown in Fig. 2, the carrier with the circular cross-section shape could obtain obviously stronger signal than that with the square shape of the same area. For example, with the area of 19.63 mm^2, signal of Al was 1.6 times larger while 1.7 times larger for Si. Therefore, porous cage carrier with circular cross-section would be used in priority. For carriers with the same cross-section area but different shape, both the equivalent internal resistance and exposed discharge area of the same amount of sample were the same. The difference in signal intensity might result from the difference in plasma distribution, which was induced by the different potential distribution surrounding the carriers with different cross-section shape. The effect of geometry shape on the potential distribution was also investigated by comparing the pin-shaped samples with disk-shaped samples in previous study.[30] Furthermore, it was also indicated that for the two kinds of cross-section shape, with the area increased, the signal intensity of the matrix elements increased firstly and then decreased. Specifically, maximum intensities could be obtained for these two cross-section geometries when the area was 19.63 mm^2. It should be noted that even with the area of 38.47 mm^2, the carrier with circular cross-section could obtain the signal that was still strong enough for the analysis ($I_{Al}=7.75\times10^{-12}$ A, $I_{Si}=7.56\times10^{-12}$ A). Therefore, the carrier with circular cross-section in the area from 20 to 38 mm^2 would be used for the dc-GD-MS analysis. According to our previous study, it is possible that difference in signal intensity between SiO_2 and Al_2O_3 might be caused by their different bond energy (799 kJ/mol vs. 512 kJ/mol).

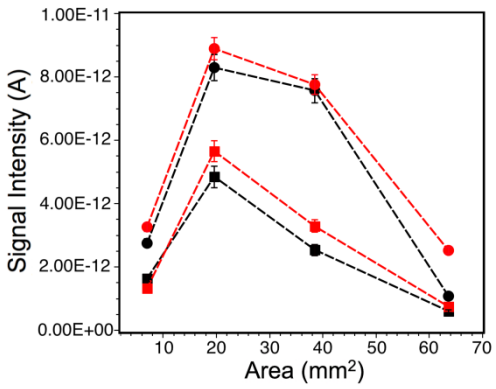

Fig. 2 Influence of shape and area of the carrier cross-section on signal intensity for SiO_2 and Al_2O_3 matrices (applied carrier length of 15 mm with Φ2 mm holes, applied discharge pressure 3.8 mPa and discharge voltage 2.0 kV, –●– and –■– stand for the signal of Si measured by carriers in circular and square cross-section respectively, –●– and –■– stand for the signal of Al measured by carriers in circular and square cross-section respectively).

Then, porous cage carriers in a series of length (15, 17, 19, 21 mm) were used to evaluate the effect of length on the

signal intensity as shown in Fig. 3, where the cross-section area was always set at 20 mm^2. As seen in the figure, both the signal intensity of Si and Al steadily decreased from 8×10^{-12} to 2×10^{-13} A with the length increased from 15 to 21 mm. In our experiment, it was found that the discharge current decreased with the increase of carrier length. It was possible that as the carrier length increased, less ionization collisions could take place, yielding a lower production of electrons and ions, and thus a lower electrical current. Meanwhile, as the carrier length increased, the distance between the tip of the sample and the ion exit slit decreased, which would lead the exist slit away from the phase boundary of the negative glow region, which resulted in less ions pass.[31] In the previous reports, the influence of the sample-exit slit distance on the analytical results was also investigated, and it was found that in the direct current (dc) mode, the signal intensity decreased with shorter sample-exit slit distances.[30, 32] In our study, the signal intensity of SiO_2 and Al_2O_3 were both above 6.59×10^{-12} A with the carrier lengths shorter than 17 mm and sufficient for the dc-GD-MS analysis. Therefore, porous cage carrier within length of 15 to 17 mm would be chose when both signal intensity and sample size were taken into account.

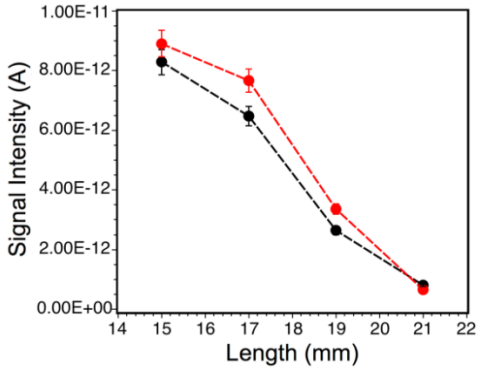

Fig. 3 Influence of carrier length on signal intensity for SiO_2 and Al_2O_3 matrices (applied carriers with Φ2 mm holes, applied discharge pressure 3.8 mPa and discharge voltage 2.0 kV, –●– and –●– stand for the signal of Si and Al measured by carriers in circular cross-section respectively).

Finally, the influence of hole size of carrier on the signal intensity were indicated in Fig. 4, where cross-section area and length were fixed at 20 mm^2 and 15 mm, respectively. The intensity of the two samples increased firstly and then decreased with hole size increased from Φ1 to Φ3 mm, revealing a "volcano" evolution trend. The signal intensity could be influenced by both the exposed area and the conductivity of the samples. With the hole size increased, the exposed area of the sample increased while the conductivity benefited from the deposition of tantalum cathode decreased. Due to the inverse relation between the two factors, the "volcano" evolution trend was taken for granted. Since the intensity could reach up to no less than 7×10^{-12}A within the range of Φ1.5-Φ2 mm and meet the test requirements, the practical hole size of the porous cage carrier would be chosen on account of both the signal intensity and sample size.

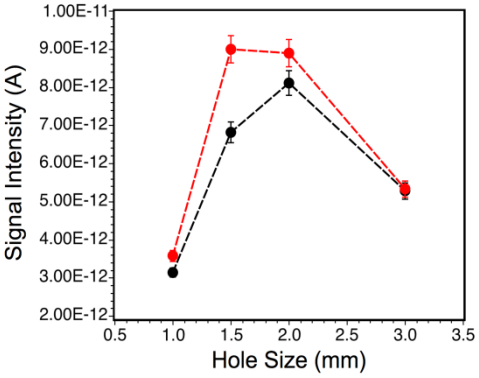

Fig. 4 Influence of carrier hole size on signal intensity for SiO_2 and Al_2O_3 matrices (applied discharge pressure 3.8 mPa and discharge voltage 2.0 kV, –●– and –●– stand for the signal of Si and Al measured by carriers in circular cross-section respectively).

3.3 Possible mechanism for sputtering and ionization of the porous cage carrier method

For this porous cage carrier method, the tantalum acted as auxiliary cathode. A possible sputtering and ionization process of this innovative porous cage carrier was proposed. The most important step was that the porous cage cathode made of tantalum was sputtered and redeposited on the sample surface which exposed to the glow discharge. As time went on, this process could result in the formation of a conducting film on the surface of the exposed sample. Consequently, this exposed area would also attract bombarding ions, and a co-sputtering process of the conducting film and the analyte ions would take place. After the subsequent ionization, the representative components of the sample could be obtained for a better analysis.

3.4 Applications of the porous cage carrier method for the soil analysis

3.4.1 Comparison with two tablet-pressed methods

In order to investigate the advantages of the porous cage carrier method, another two tablet-pressed methods were introduced to analyze the soils for comparison. One of the two methods was to press the soil into a tablet with boric acid backed, which was conventionally used in XRF. In order to ensure the tablets to be pressed into certain shape and have enough mechanical strength to avoid cracking during long-time discharge, the weight ratio of baric acid to soil needed to reach up to 5:1, making the compacted tablets about 2.8 mm thick in our study. Due to the poor conductivity, the prepared samples were analyzed by GD-MS in magnetic-enhanced radio frequency mode developed in our group.[33] However, signal intensity related to the detection limit was too low to meet the analysis requirement due to loss of the rf power with the thick tablets (Fig. 5).[34] To improve the signal intensity, another method with soils pressed onto a pure indium sheet was also

attempted. As shown in Fig. 5, the signal intensity could be increased to 2.54×10^{-12}A in rf mode. However, the signal gradually decreased due to the little amount of soil attached on the indium sheet despite which might cause the stable discharge retaining for a short time. Compared with these two methods, the porous cage carrier method was not restricted by the geometric shape of the sample. The introduced sample needed only a small amount of soils matching the carrier size, which could be easily achieved by rough mechanical press. By using the porous cage carrier method, the signal intensity could reach up to 3.76×10^{-12}A in a dc mode (Fig. 5), leading to much more lower detection limits (e.g. 0.014 μg g^{-1} for Tb), stable discharge could be retained for more than 100 mins, and the prepared samples could even be used repeatedly until they almost run out. Furthermore, as shown in Fig.6 (the signal for the boric acid method shown in the figure was amplified a hundred times), the interference peaks closed to the Si peak exhibited by using the two tablet-pressed methods, which might be produced from the reaction between C, N and O in soils during discharge process, and could be effectively suppressed by using the porous cage carrier method. It might because Ta acted as a good "getter" to C, N and O.[35] Moreover, the Ta carrier could also reduce the interferences of $^{115}In^{24}Mg$, $^{115}In^{25}Mg$, $^{115}In^{36}Ar$, $^{115}In^{40}Ar$ for the determination of rare earth elements. Therefore, it could be concluded that the porous cage carrier method has greatly improved the capability of soil analysis by GD-MS.

3.4.2 Analytical performance

3.4.2.1 Optimization of discharge parameters

Discharge parameters, namely, the discharge pressure and the discharge power (discharge voltage & discharge current) were optimized. The discharge pressure was optimized in the range 1.3-6.8mPa. The optimal value, providing maximal intensities, was found to be 4.5 mPa.

In this work, the relationship between the discharge power and the ion intensity of Si matrix using this porous cage carrier method was examined with reference material GBW07390. The optimal discharge power value, providing maximal intensities, was found to be 2.0 kV and 1.8 mA. During the pre-sputtering stage, the signal of matrix element Si increased gradually with the gradual decrease of interferences peaks from C, N, O, H at the same time. Stable signal intensity could be obtained after continuous pre-sputtering for 20 mins, where the signal intensity of Si could reach 3.76 $\times10^{-12}$ A. When the voltage exceeded 2.0 kV, the signal strength of the Si decreased rapidly, and the interference peaks formed by C, N, O, and H increased. This might be because the organic matter in the soil was excited and sputtered when the voltage exceeded 2.0 kV, resulting in the amount of C, N, O and H increased in plasma.

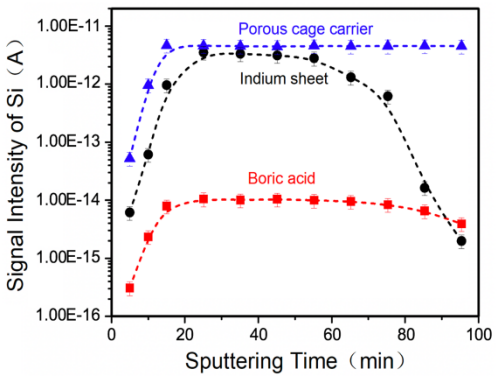

Fig. 5 The intensity changes of Si matrix of the soils as time went on (applied discharge pressure 4.5 mPa and discharge voltage 2.0 kV).

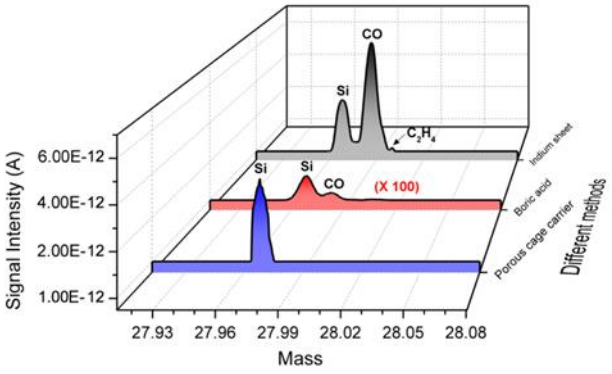

Fig. 6 Interference peaks closed to the Si peak exhibited by using the three methods (applied discharge pressure 4.5 mPa and discharge voltage 2.0 kV).

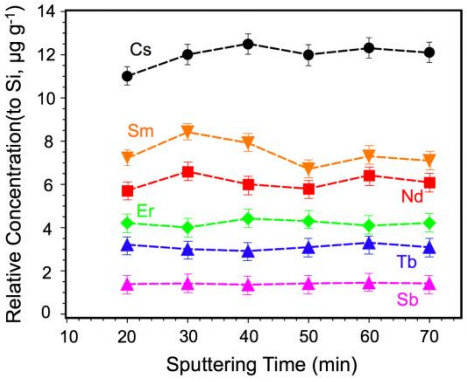

Fig. 7 Stability of the discharge, represented by the raw concentration of six selected trace elements, as measured during sputtering of the reference material GBW07390.

3.4.2.2 Stability, precision and reproducibility.

Table 1 Trace elements composition of dc-GD-MS non-RSF-corrected results for reference materials GBW07390 and GBW07401 (relative to Si)

Element	GBW07390			GBW07401			RSF	
	Certified value (μg g^{-1})	Measured value (μg g^{-1})	RSF_1	Certified value (μg g^{-1})	Measured value (μg g^{-1})	RSF_2	RSF_{M-S}	RSF_S
Cs	8.6±0.4	12 (8.3)	0.72	9.0±0.7	9.8 (5.5)	0.91	0.82	/
La	40±2	116 (7.0)	0.34	34±2	89 (11)	0.38	0.36	1.39
Pr	9.0±0.4	9.6 (4.5)	0.94	7.5±0.5	6.3 (3.6)	0.87	0.91	/
Nd	35±1	6.1 (6.4)	5.74	28±2	7.4 (13)	3.78	4.76	0.25
Yb	2.8±0.2	3.2 (5.0)	0.88	2.7±0.3	4.2 (6.9)	0.64	0.76	/
Ga	19.2±0.7	23 (2.0)	0.83	19.3±1.1	23 (5.4)	0.84	0.83	/
Sm	6.5±0.3	7.5 (8.8)	0.87	5.2±0.3	4.6 (5.9)	1.13	1.00	/
Eu	1.4±0.1	1.3 (3.2)	1.08	1.0±0.1	1.3 (7.4)	0.77	0.93	/
Tb	0.91±0.05	3.1 (5.2)	0.29	0.75±0.06	2.8 (14)	0.27	0.28	/
Dy	5.0±0.4	7.3 (5.8)	0.68	4.6±0.3	11 (5.2)	0.42	0.55	/
Ho	1.00±0.09	1.2 (8.3)	0.83	0.87±0.07	0.57 (2.7)	1.53	1.18	/
Hf	5.0±0.3	7.9 (4.5)	0.63	6.8±0.8	9.2 (12)	0.74	0.69	/
Ce	74±3	156 (2.9)	0.47	70±4	128 (5.1)	0.55	0.51	1.15
Gd	5.5±0.3	33 (4.8)	0.17	4.6±0.3	41 (9.4)	0.11	0.14	/
Er	2.8±0.2	4.2 (3.8)	0.67	2.6±0.2	4.1 (5.9)	0.63	0.65	/
Tm	0.44±0.03	0.14 (11)	3.14	0.42±0.06	0.10 (6.5)	4.20	3.67	/
Lu	0.43±0.03	0.32 (3.1)	1.34	0.41±0.04	0.32 (6.8)	1.28	1.31	/
Th	12.8±0.5	8.5 (3.9)	1.51	11.6±0.7	9.1 (5.3)	1.27	1.39	/
U	2.3±0.2	2.6 (3.9)	0.88	3.3±0.4	3.6 (15)	0.92	0.90	/
Sn	3.2±0.2	2.3 (8.3)	1.39	6.1±0.7	5.6 (3.2)	1.09	1.24	2.36
Sb	1.08±0.09	1.4 (2.2)	0.77	0.87±0.21	1.1 (7.3)	0.79	0.78	2.89

Measured concentration determined from ion beam ratios.

Values in the "( )" represent the RSD of five measurements for each trace elements.

RSF_{M-S} was the average values of RSF_1 and RSF_2 values obtained by reference materials GBW07390 and GBW07401.

RSF_S was the "standard" RSF values supplied by the commercial Autoconcept GD90 software.

"/" means no correspond data can be found in the Autoconcept GD90 database.

The stability, precision and reproducibility of analysis of trace elements in the soil were investigated. The relative concentrations of six typical elements including Cs, Sm, Nd, Er, Tb, Sb in reference material GBW07390 were selected to plot against time as shown in Fig. 7. It could be seen that the relative concentration changed little throughout the whole analysis process, indicating that the sputtering and atomization of the soil could be remained stable by using this porous cage carrier. It could be further revealed by the internal precisions of 21 trace elements of the reference material GBW07390 and GBW07401 as shown in Table 1, which was 16% and 15% RSD (n=5) respectively. Moreover, the external precisions of these elements were better than 20% for both two samples. These results indicated that the analysis of soils by using this method was reproducible.

The relative sensitivity factor (RSF) values, which was determined from the analysis of the standard reference materials of similar matrix composition, was crucial to correct the measured values into accurate quantitative values. Therefore, the RSF values were firstly calculated by using the reference materials GBW07390 and GBW07401 according to the definition RSF = (real concentration) / (measured concentration).[36,37] All the RSF values were determined relative to Si and listed in Table 1. "Matrix specific" RSF values of each element could be further obtained by averaging the two corresponding RSF values of reference materials GBW07390 and GBW07401. To evaluate the accuracy of "matrix specific" RSF values, they were used to determine several trace elements in the third reference material GBW07430. As shown in Table 2 and Fig. 8, it revealed that the calculated values were in good agreement with the certified values, leading the relative errors in a range from 0.7% to 17%. By contrast, when correcting the measured values by using the "standard" RSF values supplied by the commercial Autoconcept GD90 software, which was determined from a variety of metals and alloys, the errors exceeded 85%. These results indicated that better accuracies could be attained with the "matrix-specific" RSF values.

Table 2 Comparation of dc-GD-MS results of reference material GBW07430 calibrated by RSF (relative to Si), the LA-ICP-MS results and the certified values

Element (GBW07430)	Certified value (μg g^{-1})	Measured value (μg g^{-1})	RSF_S adjusted value (μg g^{-1})	Error (%)	RSF_{M-S} adjusted value (μg g^{-1})	Error (%)	LA-ICP-MS value (μg g^{-1})	Error (%)
Cs	13.9±0.7	17(7.5)	/	/	13.8	-0.7	12(15)	-14
La	67±3	171(5.4)	238	255	61	-8.9	49(12)	-26
Pr	14.6±1.1	17(4.9)	/	/	15.4	5.5	13(9.8)	-11
Nd	57±4	11(8.5)	2.75	-95	52	-8.7	46(11)	-19
Yb	3.8±0.2	4.8(8.3)	/	/	3.6	-5.3	2.9(16)	-24
Ga	25.1±1.2	34(7.5)	/	/	28.2	12	27(9.3)	7.6
Sm	10.4±0.5	9.9(3.7)	/	/	9.9	-4.8	9.3(20)	-11
Eu	1.66±0.07	1.68(4.5)	/	/	1.56	-6.0	1.43(18)	-14
Tb	1.3±0.1	5.1(7.1)	/	/	1.4	7.7	1.2(6.9)	-7.7
Dy	7.4±0.5	12(9.8)	/	/	6.6	-11	6.1(15)	-18
Ho	1.41±0.08	1.4(12)	/	/	1.65	17	0.98(17)	-30
Hf	8.2±0.4	11(6.5)	/	/	7.59	-7.4	3.4(23)	-59
Ce	133±5	295(3.8)	339	155	150	13	121(16)	-9.0
Gd	8.5±0.7	55(7.9)	/	/	7.7	-9.4	6.4(27)	-25
Er	3.8±0.2	6.3(3.6)	/	/	4.1	7.8	3.4(9.4)	-11
Tm	0.57±0.05	0.16(14)	/	/	0.59	3.5	0.48(19)	-16
Lu	0.58±0.05	0.45(8.1)	/	/	0.60	3.4	0.42(7.2)	-28
Th	28±2	21(7.4)	/	/	29	3.6	15(6.6)	-46
U	5.9±0.3	7.2(9.3)	/	/	6.5	9.8	2.6(8.9)	-56
Sn	12.4±0.8	9.7(12)	23	85	12.0	3.3	5.2(4.9)	58
Sb	1.9±0.2	2.7(6.2)	7.8	311	2.1	11	1.6(19)	-16

Measured concentration determined from ion beam ratios.
Values in the "( )" represent the RSD of five measurements for each trace elements.
RSF_{M-S} was the average values of RSF_1 and RSF_2 values obtained by reference materials GBW07390 and GBW07401.
RSF_S was the "standard" RSF values provided by the commercial Autoconcept GD90 software.
"/" means no correspond data can be found in the Autoconcept GD90 database or calculated accordingly.

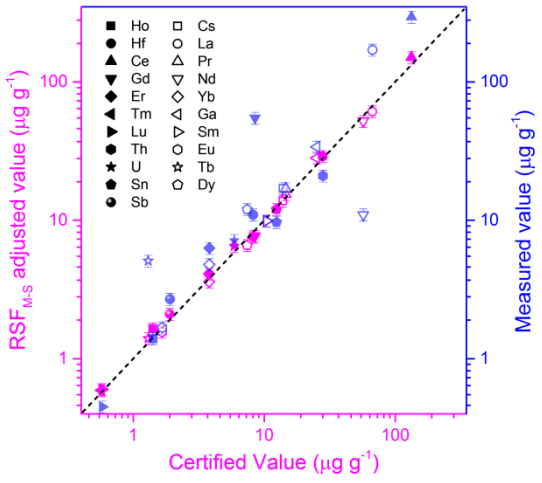

Fig. 8 Certified concentrations vs measured concentrations and RSF_{M-S} adjusted values for elements in the reference material GBW07430.

Furthermore, LA-ICP-MS was also applied for the further comparison with detecting reference material GBW07430. Table 2 indicated that the relative error of 20 of 21 elements concentrations determined by dc-GD-MS tantalum carrier method was within 13%. However, 15 of 21 elements concentrations determined by LA-ICP-MS was in the range of 14-59%. Meanwhile, the reproducibility of LA-ICP-MS was also worse than that obtained by dc-GD-MS with the porous cage carrier method. Furthermore, the results confirmed that the dc-GD-MS porous cage carrier method was more suitable for analyzing the soil and the similar samples.

Limits of detection (LOD) of the porous cage carrier method was roughly evaluated by using the reference material GBW07390. According to the IUPAC definition, the LOD can be calculated by LOD=$3\sigma_b/m$. σ_b was the standard deviation of the background around the analyte peak in the range of 20 times the width at half-height of the peak.[38,39] The detection sensitivity $m=(I_p-I_b)/C_X$, where I_p was the average ion intensity of the element to be tested, I_b was the average ion intensity of

the background position, and C_X was the concentration of the tested element. As shown in Table 3, the detection limit of Tb obtained by this porous cage carrier method could reach 0.014 μg g^{-1}, which indicated that the porous cage carrier method was qualified for the analysis of trace elements in soils.

Table 3 Detection limits of 21 trace elements in reference material GBW07390 (relative to Si)

Element	LOD（μg g^{-1}）	Element	LOD（μg g^{-1}）
Cs	0.12	Hf	0.19
La	0.16	Ce	0.25
Pr	0.31	Gd	0.13
Nd	0.83	Er	0.04
Yb	0.42	Tm	0.087
Ga	0.09	Lu	0.041
Sm	1.31	Th	0.90
Eu	0.16	U	0.19
Tb	0.014	Sn	0.30
Dy	0.21	Sb	0.040
Ho	0.13	/	/

4. Conclusions

In the present work, a porous cage carrier method was developed to analyze the trace elements in soils by dc-GD-MS. The influence of geometric and dimensional factors on the signal intensity has been studied sequentially. It was shown that porous cage carriers with circular cross-section area in the range from 20 to 38 mm^2, length from 15 to 17 mm and diameter of hole size from 1.5 mm to 2.0 mm could obtain good signals, where the practical parameters should be determined on account of the measurement requirement such as sample size. Then the method was applied to the analysis of trace elements in soil reference materials. The internal precision was obtained within 16%, the external precision was better than 20% and the relative error was in the range from 0.7% to 17% indicated the good stability, reproducibility and accuracy of this method in soil analysis, respectively. After calibration by the “matrix-specific” RSF, the accuracy and reproducibility of dc-GD-MS results were better than the LA-ICP-MS. The detection limit of Tb could reach 0.014 μg g^{-1}, which made this method qualified for the analysis of trace elements in soils. By comparing with the conventional tablet-pressed methods, the porous cage carrier method could be recognized as an easier established method for soil analysis with more convenient sample preparation, good stability, reproducibility and better detection limit. The development of this method would promote the further application of GD-MS in the environmental area.

Conflicts of interest

There are no conflicts to declare.

Acknowledgements

The authors greatly acknowledge the financial support by the National Natural Science Foundation of China (Grant No. 21775156), Shanghai foundation for new research methods (Grant No. 17142201600), Intergovernmental International Cooperation Project of Shanghai Science and Technology Commission (Grant No. 19520712000), Project of the Technology Center, Shanghai Tobacco (Group) Corporation (Grant No. K2018-1-056p).

References

1 Y. L. Lee, C. C. Chang and S. J. Jiang, *Spectrochim. Acta, Part B*, 2003, **58**, 523-530.
2 A. Kumari, R. Panda, M. K. Jha, J. R. Kumar and J. Y. Lee, *Miner. Eng.,* 2015, **79**, 102-115.
3 L. M. Li, J. Wu, J. Lu, X. Y. Min, J. Xu and L. Yang, *Ecotoxicol. Environ. Saf.*, 2018, **166**, 345-353.
4 G. Huang, L. Wang, Z. Sun, X. Li, Q. Zhou and X. Huang, *Biol. Trace. Elem. Res.*, 2014, **163**, 224-34.
5 S. J. Ramos, G. S. Dinali, C. Oliveira, G. C. Martins, C. G. Moreira, J. O. Siqueira and L. R. G. Guilherme, *Curr. Pollut. Rep.*, 2016, **21**, 28-50.
6 X. F. Li, Z. B. Chen, Z. Q. Chen and Y. H. Zhang, *Chemosphere*, 2013, **93**, 1240-1246.
7 B. G. Wei, Y. H. Li, H. R. Li, J. P. Yu, B. X. Ye and T. Liang, *Ecotoxicol. Environ. Saf.*, 2013, **96**, 118-123.
8 N. Zhang, Ch. Huang and B. Hu, *Anal. Sci.*, 2007, **23**, 997-1002.
9 G. L. Han, Z. L. Song and Y. Tang, *Can. J. Soil Sci.*, 2017, **97**, 606-612.
10 B. Zawisza, K. Pytlakowska, B. Feist, M. Polowniak, A. Kita and R. Sitko, *J. Anal. At. Spectrom.*, 2011, **26**, 2373-2390.
11 E. H. Evans, J. Pisonero, C. M. M. Smith and R. N. Taylor, *J. Anal. At. Spectrom.*, 2019, **34**, 803-822.
12 H. M. Anawar, M. C. Freitas, N. Canha, I. Dionisio, H. M. Dung, C. Galinha and A. M. G. Pacheco, *J. Radioanal. Nucl. Chem.*, 2012, **294**, 377-381.
13 I. A. Alnour, H. Wagiran, N. Ibrahim, S. Hamzah, B. S. Wee and M. S. Elias, *J. Radioanal. Nucl. Chem.*, 2015, **303**, 1999-2009.
14 J.Q. McComb, C. Rogers, F.X. Han and P.B. Tchounwou, *Water, Air Soil Pollut.*, 2014, **225**, 2169-2179.
15 Y. S. Liu, Z. C. Hu, M. Li and S. Gao, *Chin. Sci. Bull.*, 2013, **58**, 3863-3878.
16 D. C. Duckworth, C. M. Barshick, D.A. Bostick and D.H. Smith, *J. Anal. At. Spectrom.*, 1993, **47**, 243-245.
17 D. C. Duckworth, C. M. Barshick and D.H. Smith, *J. Anal. At. Spectrom.*, 1993, **8**, 875-879.
18 J. Teng, C. M. Barshick, D. C. Duckworth, S. J. Morton, D. H. Smith and F. L. King, *Appl. Spectrosc.*, 1995, **49**, 1361-1366.
19 M. Betti, S. Giannarelli, T. Hiernaut, G. Rasmussen and L. Koch, *Fresenius. J. Anal. Chem.*, 1996, **355**, 642-646.
20 D. C. Duckworth, D. L. Donohue, D. H. Smith, T. A. Lewis and R. K. Marcus, *Anal. Chem.*, 1993, **65**, 2478-2484.
21 A. Ganeev, A. Titova, B. Korotetski, A. Gubal, N. Solovyev, A. Vyacheslavov, E. Iakovleva and M. Sillanpää, *Anal. Lett.*, 2019, **52**, 671-684.
22 A. Ganeev, O. Bogdanova, I. Ivanov, B. Burakov, N. Agafonova, B. Korotetski, A. Gubal, N. Solovyev, E. Iakovleva and M. Sillanpaa, *RSC Adv.*, 2015, **5**, 80901-80910.

23 W. Schelles and R. Van Grieken, *J. Anal. At. Spectrom.*, 1997, **12**, 49-52.
24 V. Hoffmann, M. Kasik, P.K. Robinson and C. Venzago, *Anal. Bioanal. Chem.*, 2005, **381**, 173-188.
25 J. Pisonero, B. Fernández and D. Günther, *J. Anal. At. Spectrom.*, 2009, **24**, 1145-1160.
26 M. Bouza, R. Pereiro, N. Bordel, A. Sanz-Medel and B. Fernández, *J. Anal. At. Spectrom.*, 2015, **30**, 1108-1116.
27 B. C. Zhao, W. Hang and B. L. Huang, *Chin. J. Inorg. Anal. Chem.*, 2011, **01**, 13-23.
28 J. L. Dong, R. Qian, W. Xiong, H. Y. Qu, B. Siqin, S. J. Zhuo, J. Jin, Z. Y. Wen, P. He and P.K. Robinson, *Int. J. Mass Spectrom.*, 2014, **361**, 1-8.
29 B. Siqin, R. Qian, S. J. Zhuo, J. Gao, J. Jin and Z. Y. Wen, *J. Anal. At. Spectrom.*, 2014, **29**, 2064-2071.
30 A. Bogaerts and R. Gijbels, *J. Am. Mass. Spectrom.*, 1997, **8**, 1021-1029.
31 M. Saito, *Anal. Chim. Acta.*, 1993, **274**, 327-334.
32 S. De Gendt, R. Van Grieken, W. Hang and W. W. Harrison, *J. Anal. At. Spectrom.*, 1995, **10**, 689-695.
33 J. Wei, J. L. Dong, S. J. Zhuo, R. Qian, Y. X. Fang, Q. Chen and E. Patel, *Anal. Chem.*, 2017, **89**, 1382-1388.
34 N. Jakubowski, R. Dorka, E. Steers and A. Tempez, *J. Anal. At. Spectrom.*, 2007, **22**, 722-735.
35 Y. Mei and W. W. Harrison, *Spectrochim. Acta Part B*, 1991, **46**, 175-182.
36 R. K. Marcus and J. A. C. Broekaert, Glow Discharge Plasmas in Analytical Spectroscopy, John Wiley & Sons, Chichester, 2003.
37 R. Qian, S.J. Zhuo, Z. Wang and P.K. Robinson, *J. Anal. At. Spectrom.*, 2013, **28**, 1061-1067.
38 I. Rauschenbach, E. K. Jessberger, S. G. Pavlov, S. Schröder and H. -W. Hübers, 41th Lunar and Planetary Science Conference (2010), 1658.
39 A. Shrivastava, V. B. Gupta, *Chron. Young Sci.*, 2011, **2**, 21-25.